Geological Survey of Canada
Commission géologique du Canada

PAPER 87-21

BASIC VOLCANICS IN THE HASSEL FORMATION (MID-CRETACEOUS) AND ASSOCIATED INTRUSIVES, ELLESMERE ISLAND, DISTRICT OF FRANKLIN, NORTHWEST TERRITORIES

K.G. OSADETZ
P.R. MOORE

Canada

1988

GEOLOGICAL SURVEY OF CANADA
PAPER 87-21

BASIC VOLCANICS IN THE HASSEL FORMATION (MID-CRETACEOUS) AND ASSOCIATED INTRUSIVES, ELLESMERE ISLAND, DISTRICT OF FRANKLIN, NORTHWEST TERRITORIES

K.G. OSADETZ
P.R. MOORE

1988

Energy, Mines and Resources Canada
Énergie, Mines et Ressources Canada

Available in Canada through

authorized bookstore agents and other bookstores

or by mail from

Canadian Government Publishing Centre
Supply and Services Canada
Ottawa, Canada K1A 0S9

and from

Geological Survey of Canada offices:

601 Booth Street
Ottawa, Canada K1A 0E8

3303-33rd Street N.W.
Calgary, Alberta T2L 2A7

Cat. No. M44-87/21E Canada: $5.00
ISBN 0-660-12769-5 Other countries: $6.00

Price subject to change without notice

For description of cover photo
see page 5.

Critical readers

A.F. Embry
B.D. Ricketts
W.R.H. Baragar

Authors' addresses

K.G. Osadetz
Institute of Sedimentary and Petroleum Geology
3303 - 33rd Street N.W.
Calgary, Alberta T2L 2A7

P.R. Moore
New Zealand Geological Survey
P.O. Box 30-368
Lower Hutt, New Zealand

Original manuscript submitted: 84-07-09
Final version approved for publication: 86-06-19

CONTENTS

Illustrations

Figures

Tables

BASIC VOLCANICS IN THE HASSEL FORMATION (MID-CRETACEOUS) AND ASSOCIATED INTRUSIVES, ELLESMERE ISLAND, DISTRICT OF FRANKLIN, NORTHWEST TERRITORIES

Abstract

Subalkaline basic volcanic rocks with tholeiitic rock series affinities are interbedded with nonmarine sandstones in the Hassel Formation (mid-Cretaceous) in the vicinity of Lake Hazen, northern Ellesmere Island. Nonmarine volcanic flows are the extrusive equivalents of a significant complex of sills and dykes that are exposed in Tertiary (Eurekan) structures between Tanquary Fiord and Lake Hazen. Two distinct low- and high-phosphorus parental olivine tholeiite magmas are identified on the basis of P_2O_5, FeO*, and TiO_2 abundances. Both parental magmas can be derived from an undepleted mantle source with a normal phosphorus abundance (P~200 ppm), by different degrees of equilibrium partial melting. The low-phosphorus parental olivine tholeiite (0.29 wt % P_2O_5) can be formed by approximately 12 per cent partial melting of the mantle source: this rock exhibits minor element characteristics similar to oceanic tholeiites. The high-phosphorus parental olivine tholeiite resulted from less than 12 per cent partial melting of a similar mantle source: it exhibits certain alkaline characteristics (high TiO_2 and P_2O_5). The low-phosphorus parental magma fractionated ~20 per cent olivine ± clinopyroxene and plagioclase. The high-phosphorus parental magma fractionated undetermined amounts of similar phases to produce derivative liquids that intruded exposed crustal levels. The low-phosphorus magma was extruded without further fractionation, while the high-phosphorus magma underwent extensive fractionation after emplacement in the rocks of the Sverdrup Basin (<2.5 km), resulting in at least one layered sill. Some flows were derived from the high-phosphorus magma late in its crystallization history, past the peak of iron enrichment. It is deduced that these basic igneous rocks represent magmatic activity within the contiguous North American – Barents Shelf craton, during the late stages of the opening of the Amerasian Basin by the anticlockwise rotation of northern Alaska and portions of northern Siberia.

Keywords: Tholeiitic rock series, phosphorus, fractionation, Cretaceous, Sverdrup Basin, Barents Shelf, Amerasian Basin.

Résumé

Des roches volcaniques basiques subalcalines ayant des affinités avec la série de roches tholéiitiques sont interlitées avec des grès non-marins de la formation de Hassel du Crétacé moyen dans les environs du lac Hazen, au nord de l'île Ellesmere. Les coulées volcaniques non-marines constituent l'équivalent extrusif d'un complexe significatif de sills et de dykes exposé dans des structures tertiaires (Eurékien) entre le fiord Tanquary et le lac Hazen. Deux magmas distincts, mais apparentés de tholéiite à olivine, dont l'un à basse teneur et l'autre à haute teneur en phosphore, sont identifiés suivant leur richesse en P_2O_5, FeO* et TiO_2. Ces deux magmas peuvent provenir d'une source en matériaux du manteau ayant une teneur normale en phosphore (P~200 ppm), mais à des degrés différents de l'équilibre de la fusion partielle. Les roches tholéiitiques à olivine apparentées à basse teneur en phosphore (0,29 wt% P_2O_5) peuvent être formées par approximativement 12% de la fusion partielle de la source mantellique: ces roches montrent des éléments caractéristiques mineurs semblables aux roches tholéiitiques marines. Les roches tholéiitiques à olivine apparentées ont une teneur élevée en phosphore et sont le résultat de moins de 12% de la fusion partielle d'une source semblable mantellique: ceci montre certaines caractéristiques alcalines (riche en TiO_2 et P_2O_5). Le magma apparenté à basse teneur en phosphore est fractionné en 20% d'olivine avec ± de clinopyroxène et de plagioclase. Le magma apparenté à haute teneur est fractionné suivant des quantités indéterminées de phases similaires produisant des substances liquides dérivées qui se sont épanchées à certains niveaux exposés de la croûte. Le magma à basse teneur en phosphore s'est épanché sans autres fractionnements au moment où le magma à haute teneur en phosphore subissait un fractionnement après son intrusion dans les roches du bassin de Sverdrup (<2,5 km), aboutissant, en dernier essor, en un sill lité. Certains écoulements provenaient, tardivement, d'un magma riche en phosphore dans sa phase de cristallisation, au-delà de sa phase la plus riche en fer. On doit en déduire que ces roches ignées basiques représentent la phase active magmatique à l'intérieur du craton Amérique du Nord - bouclier de Barents, au cours des derniers stages de formation du bassin Amérasien par la rotation rétrograde de l'Alaska septentrional et des parties septentrionales de la Sibérie.

Mots clés: série de roches tholéiitiques, phosphore, fractionnement, Crétacé, bassin de Sverdrup, bouclier de Parents, bassin Amérasien.

Introduction

Sverdrup Basin is a sedimentary basin that extends throughout much of the Queen Elizabeth Islands, District of Franklin, Northwest Territories, Canada (Fig. 1). The basin was an active site of deposition from Carboniferous through Cretaceous times. Although its internal stratigraphy is complex (Tozer, 1963; Thorsteinsson, 1974; Balkwill, 1978), two major lithostratigraphic sequences, are identifiable (Plauchut, 1971). The first sequence, representing deposition from the Early Carboniferous to the Early Cretaceous, was confined to an elliptical basin of deposition the limits of which probably lay close to the present outcrop edge of the basin. The second major sequence (comprising Lower and Upper Cretaceous strata), although conformable in central parts of the basin, transgressed the limits of the first sequence southward onto the lower Paleozoic rocks of the Arctic Platform. The second lithostratigraphic sequence can also be distinguished from the first by the presence of extensive basic magmatism in the former.

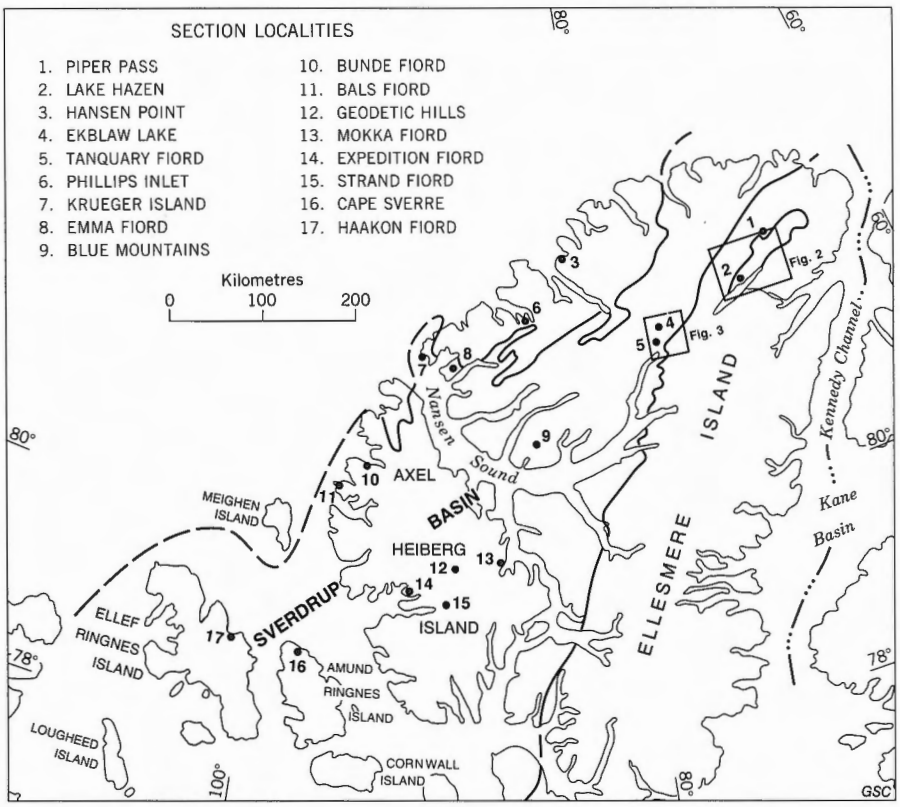

Figure 1. *Location map for the eastern Queen Elizabeth Islands.*

Sverdrup Basin was the site of episodic basic igneous activity. Small amounts of volcanic rocks were extruded during the deposition of the first lithostratigraphic sequence in the northeastern part of the basin during the Carboniferous and Permian (Thorsteinsson, 1974). In contrast, the basic magmatism accompanying the second major phase of basin subsidence produced a major component of the lithostratigraphic thickness, either as flows (Fricker, 1963; Tozer, 1963; Christie, 1964; Thorsteinsson and Trettin, 1969; Ricketts and others, 1985) or as sills and dykes (Blackadar, 1964; Balkwill, 1978; Balkwill and Fox, 1982). Volcanic rocks outcrop on: Ellesmere, Axel Heiberg, Ellef Ringnes and Amund Ringnes islands. Associated with the Cretaceous volcanic rocks is an areally more extensive suite of basic dykes and sills that occur throughout the Queen Elizabeth Islands, extending as far west as Melville Island.

Recent investigations on Axel Heiberg Island have revealed three major periods of Cretaceous volcanism in Sverdrup Basin. The oldest Cretaceous volcanic rocks occur within the Isachsen Formation [Valanginian-(?)Albian] across a wide area, extending from the Blue Mountains, north of Greely Fiord on Ellesmere Island, to Bunde Fiord on Axel Heiberg Island. This sequence of flows, entirely nonmarine, was extruded some time earlier than the onset of the long Cretaceous normal period of magnetization (P.J. Wynne, pers. comm., 1984) during the interval Valanginian to earliest Aptian. Tozer (1963) reported a 30 m thick volcanic flow at the top of the Hassel Formation (late Albian – early Cenomanian) in the Geodetic Hills on Axel Heiberg Island (Fig. 1), but subsequent geological mapping has placed this flow in the Isachsen Formation (Thorsteinsson, 1971). Another volcanic flow unit occurs below rock types typical of the lower Christopher Formation (Albian) at Mokka Fiord, on eastern Axel Heiberg Island. It is believed to be roughly correlative with volcanic rocks in the Isachsen Formation in both the Blue Mountains and Geodetic Hills. Unfortunately, the lower contact is not exposed and its exact stratigraphic position is uncertain.

The second volcanic sequence occurs within the late Albian – early Cenomanian Hassel Formation, and consists of thin flows distributed across a wide area. Volcanic flows occur within the Hassel Formation at three localities. At Lake Hazen, on northeastern Ellesmere Island, erosional remnants of volcanic flows outcrop. These flows are the subject of this paper. Other confirmed volcanic horizons in the Hassel Formation occur on northeastern Amund Ringnes Island and on eastern Ellef Ringnes Island, where Balkwill (1983) and Stott (1969) mapped thin, yet persistent, horizons of volcanic breccia and basalt flows (Fig. 1). Balkwill (1983) attributed the volcanic breccias to phreatic processes (cf. Lorenz and others, 1970), yet confirmed that both aphanitic flows and volcanic breccias were extruded on the accretionary surface of strata belonging to the informal Upper member of the Hassel Formation.

The final volcanic event occurred in early Late Cretaceous time when a thick sequence (+800 m) of nonmarine and marine volcanics and pyroclastics was extruded along the western side of Axel Heiberg Island, from Bunde Fiord to south of Strand Fiord (Ricketts and others, 1985). This sequence of volcanic rocks is assigned to the Strand Fiord Formation (?Turonian).

The basic volcanic rocks of the Lake Hazen area and the dykes and sills that were probable feeders to these flows are the subject of this paper. These rocks were extruded and emplaced during the second period of Cretaceous volcanic activity. Volcanic flows are preserved within the Hassel Formation in a Tertiary synclinorium, north and northeast of Lake Hazen (Fig. 2). At Tanquary Fiord (Fig. 3), a combination of Tertiary structure and a generally lower level of erosion than that observed at Lake Hazen, has resulted in the removal of the Hassel Formation and any flows correlative with those preserved in the Lake Hazen area.

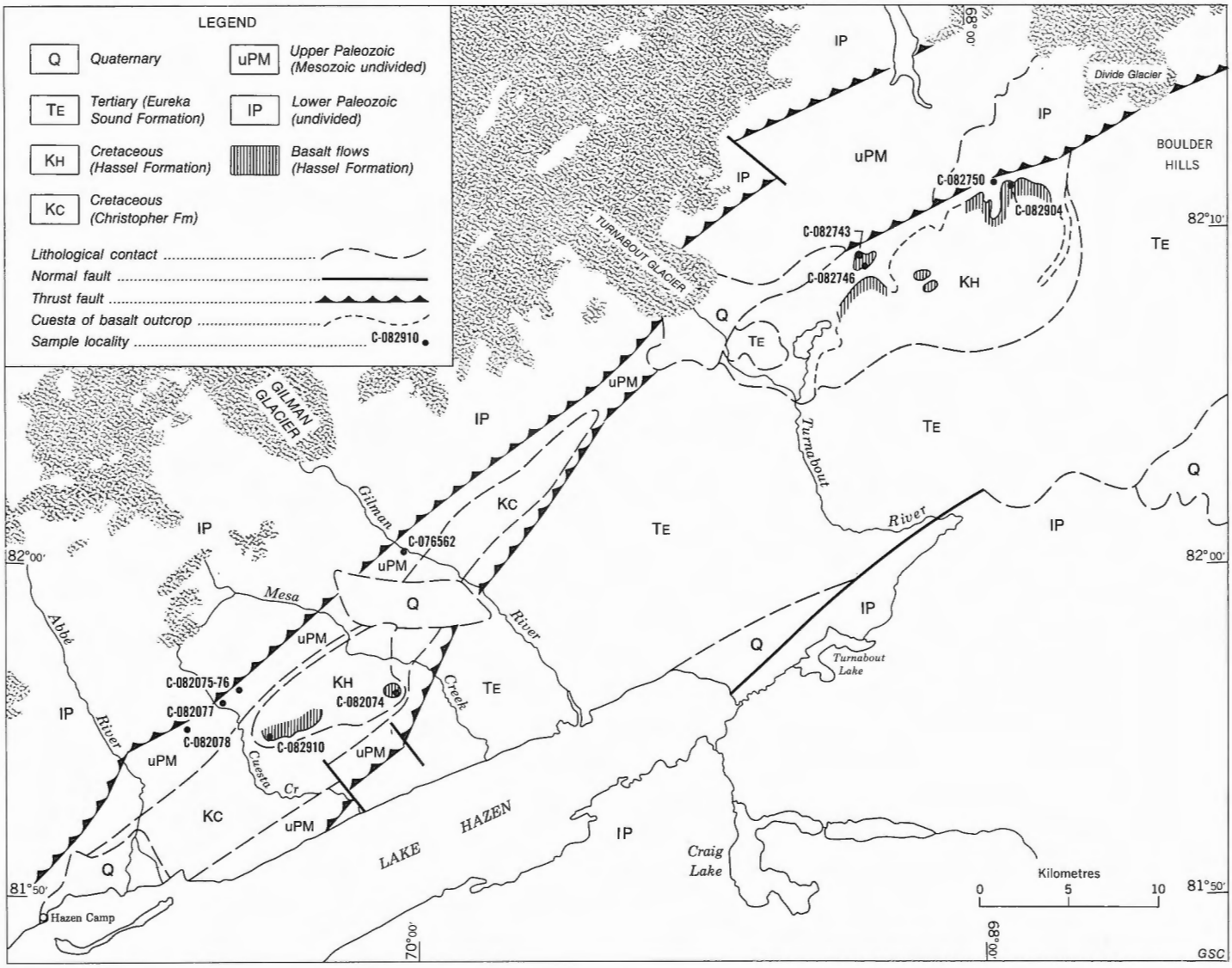

Figure 2. *Sample locality map of the Lake Hazen and Piper Pass areas indicating: simplified geological boundaries (after Trettin and others, 1982); the location of samples; and known outcrops of flows.*

The same structures result in the exposure of the sills and dykes that probably represent shallow fractionation chambers and conduits of magma to the volcanic flows. This provides a section through the intrusive-extrusive edifice, allowing an interpretation of the shallow fractionation trend of these magmas. Elucidation of the shallow fractionation trend of the magmas allows the identification of the most primitive observed compositions and the deduction of probable parental magmatic compositions, using simple models. Knowing the approximate composition of the parental magmas, it is possible to speculate that the two parental magmas were derived by differing degrees of partial melting of similar mantle source regions.

Volcanic flows

Stratigraphic setting and distribution

The Lake Hazen area occupied a basin margin setting throughout late Paleozoic and Mesozoic times. The pre-Cretaceous sequence at Lake Hazen is condensed relative to the sequences at other localities on the basin margin (Trettin and others, 1982). The succeeding Isachsen Formation (50 m) represents the limits of a major Early Cretaceous regression that affected the entire Sverdrup Basin (Plauchut, 1971; Balkwill, 1978). The Isachsen Formation is conformably overlain by thick (750 m) shales of the Christopher Formation (Trettin and others, 1982), which in turn are conformably overlain by sandstones of the Hassel Formation, representing the final coarse clastic formation of Sverdrup Basin. Younger Cretaceous beds are unknown in the Lake Hazen area. Presumably, the Tertiary Eureka Sound Formation disconformably oversteps the Hassel Formation in a similar fashion to its onlap onto lower Paleozoic strata farther to the southeast (Miall, 1979) (Figs. 2, 4c). Unfortunately, the upper limit of the Hassel Formation is commonly coincident with the present erosion surface. The contact between Cretaceous and Tertiary strata is further obscured by a combination of low dip, flat topography and lithological similarity.

Volcanic flows occur within the Hassel Formation at three main localities. Thirteen kilometres east of the snout of Turnabout Glacier a single basalt flow forms the steep

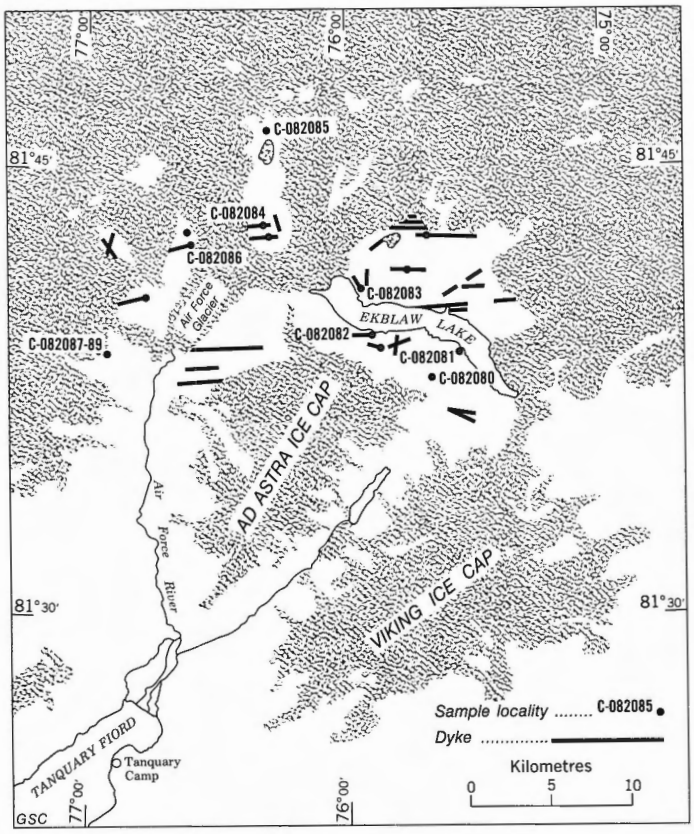

Figure 3. *Sample locality map of Tanquary Fiord and Ekblaw Lake areas, indicating the locations of samples and the outcrop and trend of dykes.*

valley walls of a small unnamed creek that flows north into the lake at the head of Piper Pass (Fig. 2). At this locality, both the base of the flow and the contact between the Hassel and the Christopher formations are exposed (Fig. 5). The present erosion surface is formed by either the flow or the sandstones of the Hassel Formation that overlie it. Six kilometres east of the snout of Turnabout Glacier, near the eastern shore of the northernmost of two small unnamed lakes, two basalt flows form a small cuesta (Figs. 2; 4a, b). The base of the lower flow is obscured and the top of the upper flow forms the present erosion surface. Other small outcrops of volcanics occur between the two localities referred to above.

Thirty-five kilometres southwest of the locality nearest Turnabout Glacier, volcanic rocks outcrop between Cuesta and Mesa creeks (Fig. 2). A single flow forms a mesa and a cuesta adjacent to these creeks (Fig. 4d). The lower contact of the Hassel Formation is exposed at these outcrops. The Hassel sandstones are in conformable and gradational contact with the underlying Christopher Formation. The flow overlies the Hassel sandstones and its upper surface forms the present erosion surface.

Thickness, environment of extrusion and correlation

At the Piper Pass locality the lowermost flow is underlain by up to 10 m of Hassel Formation sandstone (Fig. 5). The fine grained quartz sandstones are interbedded with minor siltstone and shale near the base of the formation. Coaly partings and interbeds occur near the base of the flow. Strata directly below the lower flow are interpreted as nonmarine. This flow thickens toward the east from 5 m to +26 m in the valley of the unnamed creek mentioned above. In the west, the flow is overlain by up to +20 m of fine grained, white, quartzose sandstone, similar in appearance to the underlying sandstones.

At the Turnabout Glacier locality (Fig. 6), a lower flow unit is 13 m thick. It is separated from an upper flow unit by approximately 9 m of interbedded, fine, white, quartzose sandstone, silty shale and coal. The overlying upper flow unit is +25 m thick, and may consist of up to three individual flows, as indicated by amygdule segregation bands. The nonmarine character of the underlying sediments and columnar jointing of vesicular flows suggest subaerial extrusion. However, the localized occurrence of 5 m of pillowed lava at the base of the upper flow unit (Fig. 4b) presumably represents subaqueous extrusion into a lake or stream.

The single flow unit between Mesa and Cuesta creeks is a massive, columnar jointed flow. It is approximately 2.5 to 4 m thick and is underlain by approximately 42 m of Hassel sandstones predominantly nonmarine in character.

Morphologically the flows are generally massive, columnar jointed, with vesicular and amygdaloidal tops. This, together with the nonmarine nature of the interbedded sediments, suggests a terrestrial environment of extrusion. The one exception is the pillowed lava, which is interpreted as having been extruded in a local aqueous environment. All these observations are consistent with the delta front-delta plain environment of deposition attributed to the Hassel Formation in this region (Trettin and others, 1982). At Lake Hazen volcanic flows are restricted to a delta plain setting.

Correlation amongst the three main localities is not possible. The Piper Pass flow may be the stratigraphically lowest flow because of the fact that only a thin section of sandstone underlies it. The lower flow unit at Turnabout Glacier is not correlative with the Piper Pass flow unit, on the basis of petrological considerations discussed below. It is possible that the flow between Mesa and Cuesta creeks is correlative with the upper flow unit at Turnabout Glacier, on the basis of general stratigraphic position and petrology (see below), but there is considerable uncertainty in such a correlation. The age of the Hassel Formation at Lake Hazen is determined from its general stratigraphic position: it conformably overlies Christopher Formation shale, which is dated in this area as Albian on the basis of bivalves and ammonites (Trettin and others, 1982).

Dykes and sills

Distribution, mode of intrusion and intrusive relationships

It is inferred that the flows emanate from steeply to vertically dipping dykes that occur sporadically between Piper Pass and Air Force Glacier. Dykes are most abundant at the latter locality where they form a roughly east-west trending swarm (Fig. 3). Dykes in the Lake Hazen area are less common, but have a similar trend. Several irregular intrusive bodies occur in Permo-Carboniferous strata 5 km north of the Piper Pass flows (Christie, 1964), but they have not been examined closely and their age and relationships are unknown.

Figure 4. *Photographs of volcanic flow outcrops in the Lake Hazen – Piper Pass areas. 4a: Basalt flow, Turnabout Glacier locality. 4b: Detail of pillow basalts, Turnabout Glacier locality. 4c: Basalt flow, Piper Pass locality. 4d: Basalt flow, Cuesta Creek.*

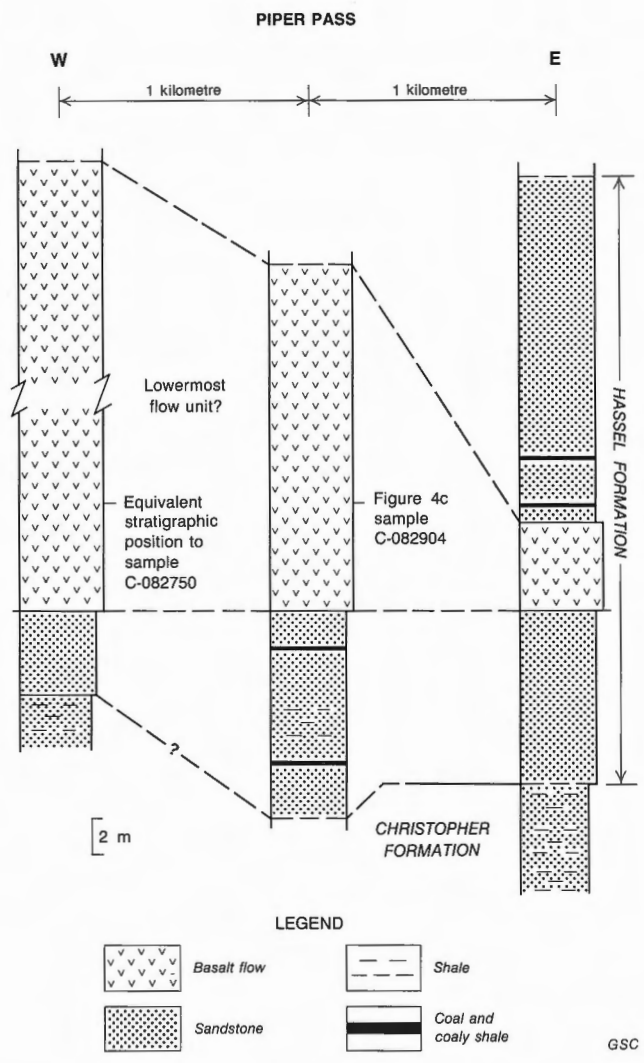

Figure 5. Stratigraphic sections of basalt flows, Piper Pass localities.

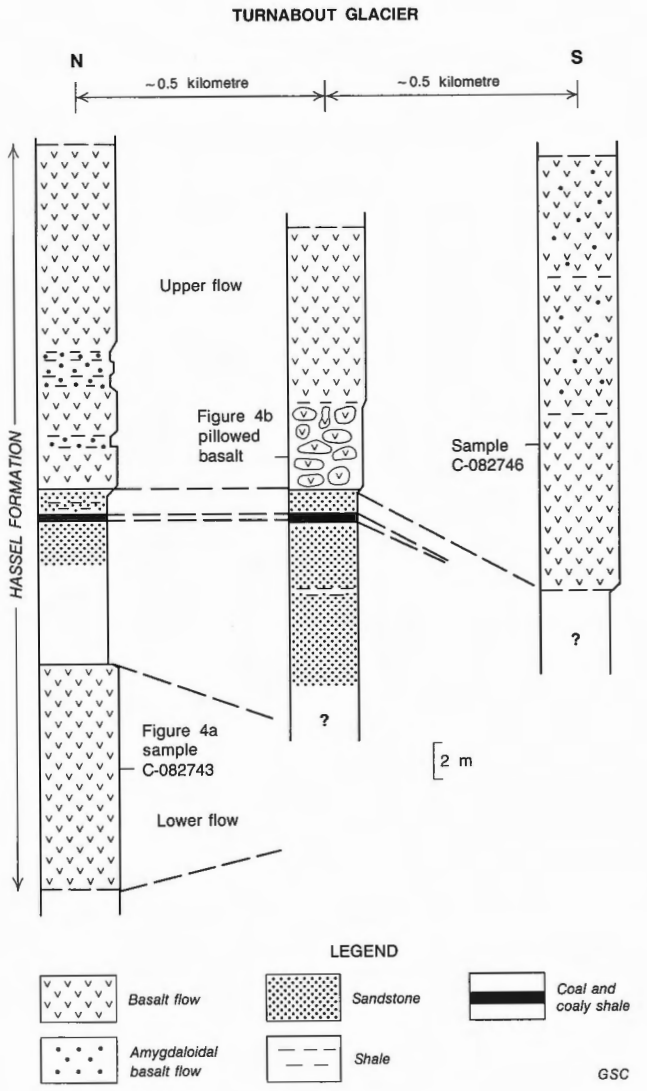

Figure 6. Stratigraphic sections of basalt flows, Turnabout Glacier localities.

Dykes are observed to cut all pre-Tertiary formations preserved in the area. They are composed of fine to medium grained diabase, basalt and porphyritic basalt. Dykes are commonly 5 km in length, and they rarely exceed one metre in width. Those observed cutting lower Paleozoic strata postdate penetrative structures attributable to the Ellesmerian Orogeny and they are considered to be coeval with dykes that intrude upper Paleozoic and Mesozoic formations. Dykes, like the sills and flows, were deformed by Tertiary orogenic activity, indicating that they predate Eurekan diastrophism.

In contrast to the flows, plutonic members of the volcanic suite can be observed to be the source of the dyke swarm, which emanates from them. Plutonic bodies generally occur as sills. At Ekblaw Lake and along the northwest limb of the Tertiary Lake Hazen Synclinorium many sills are exposed. They commonly attain thicknesses of 25 m and cover tens to perhaps several hundreds of square kilometres. Sills are generally absent from the tightly folded lower Paleozoic strata. The thickest sills occur in the sandstone and carbonate formations of the Sverdrup Basin sequence, notably the Heiberg (Triassic-Jurassic) and Isachsen (Lower Cretaceous) formations at Ekblaw Lake (Fig. 7b, c), and upper Paleozoic formations at both Lake Hazen (Fig. 7a) and on nunataks north of Air Force Glacier. Sills also occur in the fine grained clastic units, such as the Christopher and Deer Bay formations at Ekblaw Lake. This group of sills tends to be small and thin in comparison to the sills occurring in coarser grained units.

Tertiary orogeny has produced a unique section through the volcanic-intrusive complex. In excess of 5 km of pre-Tertiary strata are exposed by these structures (Osadetz, 1982). Few subvertical dykes intrude the penetratively deformed lower Paleozoic strata of the Franklinian Basin. Flat-lying sandstone and carbonate formations of the Sverdrup Basin were lifted by the ascending magma, giving rise to extensive sills at depths ranging from 1 to 2.5 km. It is evident that these sills gave rise to dykes, which are inferred to have been the conduits that extruded flows onto a Cretaceous delta plain. Apparently, flows were of the quiescent type, extruded sporadically from fissures, and over relatively limited areas. Subsequent erosion removed all effusive rocks from the Ekblaw Lake area.

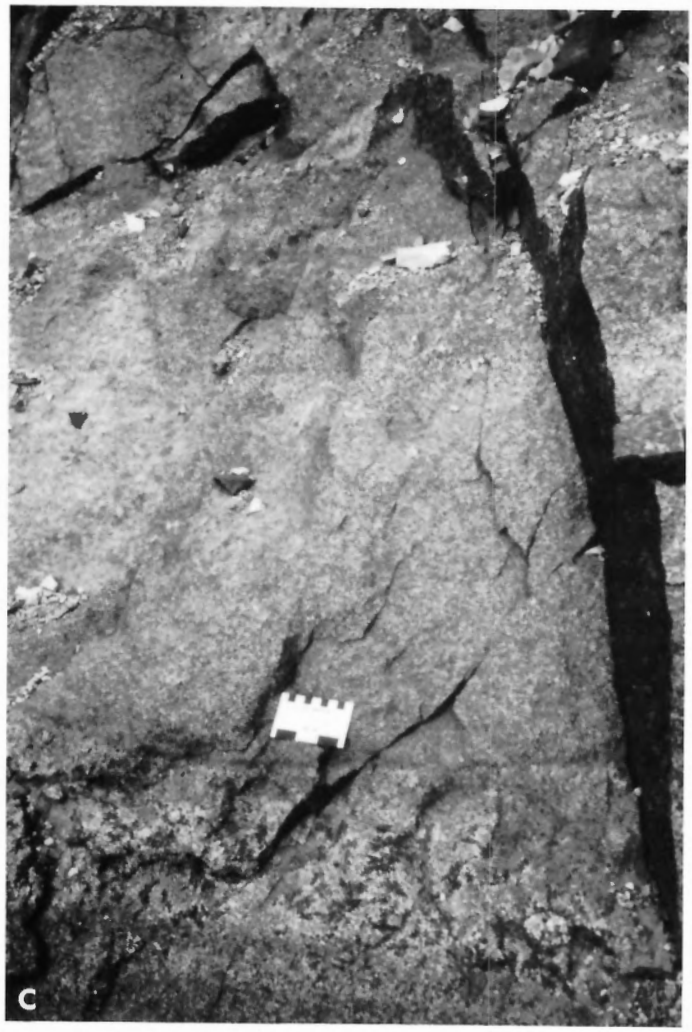

Figure 7. *Photographs of outcrops of sills intruding strata of the Sverdrup Basin. 7a: Sill intruding upper Paleozoic strata at Lake Hazen. 7b: Sills intruding the Heiberg Formation between Tanquary Fiord and Ekblaw Lake. 7c: Detail of layered sill intruding Heiberg Formation on the west side of the Air Force River valley.*

Petrography

The dykes, sills and flows of the area, although distinctive texturally, are essentially similar mineralogically. Flow rocks commonly lack glassy material and are fine grained. Dykes range from fine grained to medium grained, and one dyke at Gilman River contains glomerophenocrysts of plagioclase. Sills commonly have chilled upper and lower margins, although the lower margin is usually obscured by scree. The majority of sills examined exhibit coarse to medium grained, sub-diabasic to subophitic textures.

Primary igneous layering is rare, but is observed in one 26 m thick sill in the Heiberg Formation on the west side of the Air Force River valley (Fig. 7c). The lowermost eight metres comprise the covered lower contact and a zone of sub-diabasic texture. The central 13 m consist of coarse to very coarse grained gabbro and leucogabbro (leucocratic gabbro) with diabasic and subophitic textures; the grain size is greatest in the centre of the zone, where the texture is pegmatoid. The uppermost five metres consist of a rhythmically layered zone and upper chilled margin. Rhythmic layers have essentially the same mineralogy as the lower zones but with varying ratios of plagioclase and pyroxene producing the distinct bands. In some layers the pegmatoid texture recurs. The mechanism for development of the rhythmically layered zone is not presently understood. Samples collected from this sill help define the shallow fractionation trend of one of the magmas discussed below. Possibly this sill, or others like it, acted as a shallow fractionation chamber from which some flows were derived.

The flow unit at Piper Pass is olivine-bearing. Subhedral grains of olivine are forsteritic. They form slightly larger grains than other mineral phases. It is possible that they represent a liquidus phase that was erupted with the flow. None of the sills sampled contain modal olivine. Like the dykes and other flows they are essentially plagioclase- and clinopyroxene-rich, with ubiquitous opaque oxide phases. Most samples contain accessory, skeletal apatite grains.

Plagioclase commonly comprises 30 to 50 per cent of the rock. It is generally interpreted as the first crystallizing phase, commonly occurring as euhedral and subhedral laths. Several samples from sills exhibit ophitic textures. Rarely, anhedral clinopyroxene grains are included in larger,

euhedral, plagioclase laths. This poikilitic texture is restricted to a few, very coarse grained samples from sills; generally those intruding upper Paleozoic strata. Michel-Levy determinations suggest that compositions range from andesine to labradorite, with most compositions tending toward the more calcic end-member. Plagioclases are commonly partially saussuritized, the extent of the alteration varying from 5 to 40 per cent. Clinopyroxenes generally constitute 30 to 50 per cent of the samples. Commonly they are anhedral and, along with accessory minerals, these grains fill the interstices between plagioclase laths. Clinopyroxene is commonly colourless, pale green or greenish/brown in thin sections. One specimen from a sill in the Heiberg Formation contains slightly purplish clinopyroxene, probably titanaugite. Pyroxenes are commonly altered to either a green fibrous amphibole or a combination of yellowish fibrous amphibole and minor biotite. The alteration approaches uralitization in texture, and the amphiboles are probably generally tremolitic. Similar alteration of basic rocks is usually attributed to deuteric processes.

As mentioned above, no olivine occurs in samples collected from plutonic phases, although yellow alteration patches observed in thin sections of sill samples possibly represent pseudomorphs after olivine. Alternatively, olivine may have reacted completely with the melt during progressive crystallization.

Oxide phases are ubiquitous, commonly comprising 15 to 20 per cent of the rock. Many oxides occur as long skeletal crystals arranged in intersecting or herringbone-like patterns, but just as commonly they form euhedral and subhedral grains. High whole-rock titanium contents and the skeletal habit of many oxide grains suggest that substantial ilmenite is present. The crystallization of oxide phases appears to precede that of the pyroxenes, particularly in the flows. Considering the very high TiO_2 content of these rocks, this paragenesis is probably responsible for the lack of titanaugite in most samples. Equant grains are more likely to be magnetite and titanomagnetite. These grains exhibit a minor reddish alteration corona suggesting oxidation, again attributable to deuteric processes.

Accessory minerals include apatite, biotite, quartz and orthoclase. Apatite occurs as thin, skeletal needles in some rocks, particularly the flows. Quartz and orthoclase are uncommon; occurring as interstitial micropegmatitic intergrowths. Micropegmatite occurs in rocks of medium to coarse grain size. Generally its abundance is proportional to the grain size. It reaches almost five per cent of the mode in pegmatoid-textured leucogabbros.

Amygdules are sparsely distributed, being generally concentrated into segregation bands near the top of individual flows and the margins of hypabyssal dykes and shallow sills. Amygdules can comprise about ten per cent of the uppermost part of a flow. They also occur within the pillowed lava at the Turnabout Glacier locality. Amygdule fillings are composed of carbonate minerals and chalcedony, the former being more common.

Chemical petrology

Location and stratigraphic position of samples

Figures 2 and 3 indicate the location of igneous rock samples that were analyzed for major, minor and trace elements. Samples include specimens from all stratigraphic levels and modes of intrusion and extrusion. In all, there are ten samples of basalt flows and associated intrusives at Lake Hazen; three samples from sills in Cretaceous strata; two samples from dykes intruding the Upper Savik, Awingak and Deer Bay formations; four samples from two sills in the Heiberg Formation; and five samples from sills in upper Paleozoic strata (Tables 1, 2, 3). This suite of samples is only a reconnaissance collection of the igneous rocks present in the area. Three of the samples from the Heiberg Formation were collected from the upper marginal, lower diabasic and central subophitic zones of the layered sill mentioned above. Because of the numerous intrusions in the Heiberg Formation, samples from these sills may not be representative of the majority of sills intruding this stratigraphic level.

Analytical methods

Twenty-four samples were submitted for chemical analysis to the Geological Survey's Rock Analysis Laboratories. Major elements were analyzed by X-ray fluorescence spectroscopy (R.M. Rousseau, analyst). Additional trace elements were obtained by optical spectrometry (R.A. Meeds, analyst). Samples were submitted through Dr. Thomas Frisch and the authors are grateful for his assistance and co-operation. Analytical techniques have been discussed by Abbey (1979).

Most samples chosen for chemical analysis contained small amygdules and the analysis of some amygdaloidal rock could not be avoided (Tables 1, 2, 3). Generally, the amount of CO_2 measured in a rock during analysis is less than 2.0 weight per cent. In some cases CO_2 is substantially higher. This leads to the production of substantial normative *Cc* (calcite). Most samples have *Cc* less than 3.0 cation equivalent per cent and normative mineralogies are generally unaffected by small amounts of *Cc*. In two cases, one hypabyssal dyke and one sill, *Cc* exceeds 10.0 cation equivalent per cent and the normative mineralogies of the sample are affected. Such rocks contain normative *C* (corundum). Normative *C* in these circumstances is not related to the alumina saturation of the sample: it is an artifact of both samples with excessive carbonate amygdaloidal material and the calculations of the normative algorithm. Notwithstanding these reservations, it is observed that samples with normative *C* conform to the variation patterns observed for other samples in the suite.

Major elements

Inspection of the major element abundances indicates several general characteristics of these rocks (Tables 1, 2, 3). They are magnesium depleted and appear, generally, to be enriched in total iron (FeO*). The subalkaline nature of the rocks representing liquid compositions (flows, dykes and chilled sill margins) is illustrated by the relative abundance of alkalies in comparison to silica and the variation of these elements within the suite [Figure 8, showing the dividing line of Irvine and Baragar (1971)]. Using the basal projection of the *Cpx-Ol-Ne-Q* tetrahedron (Fig. 9), it is clear that all samples fall into the *Q'-Opx-Ab* subregion of the figure; confirming their subalkaline affinity.

Before discussing the major element variation in detail it is necessary to refer to a distinction between two groups within the suite. This distinction is most clearly exhibited by the concentration of phosphorus in these rocks (Fig. 13). It serves to distinguish a set of high-phosphorus compositions from those with less. Although the two compositional groups are also distinguished by major element variations, it is useful to refer to Figure 13 to clearly establish this distinction.

TABLE 1

Rocks approximating high-phosphorus magma composition

Analysis (wt%)	C-082087	C-082086	C-082746	C-082074	C-082743	C-082910	C-092088
SiO_2	45.42	44.35	48.97	48.29	49.50	49.63	52.70
Al_2O_3	12.38	12.53	12.28	12.38	12.60	12.62	13.13
Fe_2O_3	3.23	3.70	3.49	3.81	3.69	4.60	3.79
FeO	11.80	11.00	11.30	11.50	11.20	10.50	9.90
MgO	5.97	5.19	3.68	3.43	3.56	3.69	2.72
CaO	7.50	9.77	7.79	7.76	7.77	7.53	6.27
Na_2O	2.98	2.33	2.70	2.74	2.47	2.59	3.18
K_2O	.50	.42	1.56	1.39	1.51	1.42	2.08
TiO_2	4.15	4.17	3.25	3.28	3.26	3.24	2.45
P_2O_5	.96	.91	1.18	1.13	1.15	1.17	.91
MnO	.24	.21	.28	.30	.29	.28	.26
CO_2	.40	2.60	.20	1.40	.10	.10	0.00
H_2O	3.30	2.20	1.80	1.20	1.90	1.70	3.00
Total	98.83	99.38	98.48	98.61	99.00	99.07	100.39
Ni(ppm)	49.53	47.37	32.29	31.46	28.87	31.11	4.48
Cr(ppm)	32.71	36.84	15.62	14.61	14.43	14.44	8.96
Zr(ppm)	240	220	240	220	220	230	380
			Norm (cation equivalent)				
Q	1.619	6.185	5.892	7.367	7.666	8.466	8.111
Or	3.161	2.592	9.902	8.741	9.554	8.965	13.012
Ab	28.629	22.066	26.001	26.126	23.745	24.821	30.270
An	20.230	23.698	17.962	18.461	20.187	19.886	16.358
Di	5.015	1.908	5.352	1.910	4.758	4.786	3.614
He	3.051	1.137	5.689	2.203	5.113	4.161	4.614
En	15.108	14.149	8.213	9.091	8.152	8.489	6.157
Fs	9.191	8.434	8.731	10.489	8.759	7.381	7.861
Fo	0.000	0.000	0.000	0.000	0.000	0.000	0.000
Fa	0.000	0.000	0.000	0.000	0.000	0.000	0.000
Mt	3.613	4.074	3.906	4.234	4.136	5.136	4.197
Il	6.183	6.114	4.856	4.858	4.869	4.825	3.614
Ap	2.155	2.005	2.655	2.520	2.586	2.612	2.020
Cc	1.081	6.928	.542	3.762	.271	.270	0.000
Total	99.036	99.290	99.701	99.762	99.796	99.798	99.828

C-082087: Upper chilled margin of a layered gabbro sill intruding the Heiberg Formation on the west side of the Air Force River Valley, Tanquary Fiord area.

C-082086: Fine grained dyke intruding the Jurassic-Cretaceous sandstone and shale sequence in the Ekblaw Lake area.

C-082746: Basalt flow, upper flow unit of Turnabout Glacier locality, Lake Hazen area.

C-082074: Basalt flow southwest of Mesa Creek, Lake Hazen area.

C-082743: Basalt flow, lower flow unit at Turnabout Glacier locality, Lake Hazen area.

C-082910: Basalt flow northeast of Cuesta Creek, Lake Hazen area.

C-082088: Pegmatoid, subophitic leucogabbro in the core of a layered sill on the west side of the Air Force River Valley, Tanquary Fiord area. The same sill as C-082087.

Note: "C-" followed by a 6-digit number denotes a Geological Survey of Canada locality curated at the Institute of Sedimentary and Petroleum Geology.

TABLE 2

Rocks approximating low-phosphorus magma composition

Analysis (wt%)	C-082082	C-076562	C-082904	C-082080	C-082079	C-082090	C-082750	C-076563
SiO_2	46.28	47.80	47.29	44.26	47.73	47.07	48.31	47.34
Al_2O_3	12.76	13.16	13.44	12.78	13.53	13.34	14.82	13.26
Fe_2O_3	4.15	5.29	5.90	4.24	7.89	8.28	4.65	5.07
FeO	9.30	9.10	7.90	8.10	5.40	5.20	7.30	8.90
MgO	4.84	5.07	4.60	2.66	5.10	4.94	4.46	5.26
CaO	9.19	9.01	2.04	11.56	8.73	8.48	10.47	9.81
Na_2O	2.31	2.62	2.52	2.32	2.22	2.13	2.76	2.38
K_2O	.70	.81	.92	.67	.92	.89	.79	.78
TiO_2	3.14	3.66	3.48	3.28	3.16	3.20	2.97	3.36
P_2O_5	.39	.39	.37	.39	.42	.40	.35	.38
MnO	.20	.20	.21	.24	.17	.17	.16	.19
CO_2	4.10	.50	1.30	6.10	.80	.90	.50	.20
H_2O	1.40	2.70	2.20	3.10	3.50	3.90	2.10	2.00
Total	98.76	100.31	92.17	99.70	99.57	98.90	99.64	98.93
Ni(ppm)	51.72	48.24	41.00	40.00	41.07	44.55	52.73	47.33
Cr(ppm)	25.79	24.17	24.00	13.33	25.00	27.27	23.64	35.11
Zr(ppm)	230	220	190	210	210	240	200	200
				Norm (cation equivalent)				
Q	11.290	5.550	7.021	14.059	7.907	8.627	4.443	4.542
Or	4.323	5.047	5.777	4.155	5.844	5.704	4.864	4.875
Ab	21.618	24.831	23.935	21.948	21.350	20.776	25.998	22.724
An	17.925	22.958	23.970	17.083	25.976	26.245	26.938	24.696
Di	0.000	10.317	6.957	0.000	7.046	6.009	12.790	12.899
He	0.000	4.217	2.884	0.000	2.608	2.287	4.632	5.539
En	13.958	9.617	9.967	7.743	11.577	11.788	6.510	8.993
Fs	7.506	3.931	4.075	5.511	4.285	4.487	2.358	3.861
Fo	0.000	0.000	0.000	0.000	0.000	0.000	0.000	0.000
Fa	0.000	0.000	0.000	0.000	0.000	0.000	0.000	0.000
Mt	4.526	5.689	5.509	4.670	5.221	5.334	4.892	5.404
Il	4.571	5.377	5.129	4.809	4.718	4.841	4.329	4.978
Ap	.842	.861	.811	.867	.945	.909	.768	.848
Cc	10.828	1.334	3.480	16.250	2.168	2.470	1.325	.583
Total	97.387	99.729	99.475	97.095	99.645	99.477	99.847	99.897

C-082082: Fine grained dyke intruding the Jurassic-Cretaceous sandstone and shale sequence in the Ekblaw Lake area. Rocks of this dyke contain in excess of 10.8 cation equivalent per cent *Cc*, and *C* = 2.187 cation equivalent per cent. See discussion in the text.

C-076562: Fine grained dyke intruding the Jurassic-Cretaceous sandstone and shale sequence on the Gilman River, Lake Hazen area.

C-082904: Basalt flow, Piper Pass locality, Lake Hazen area.

C-082080: Fine grained hypabyssal sill intruding the Christopher Formation southwest of Ekblaw Lake. The sample contains in excess of 16.2 cation equivalent per cent *Cr*, and *C* = 2.645 cation equivalent per cent. See discussion in the text.

C-082079: Fine grained plagioclase glomeroporphyritic dyke intruding the Jurassic-Cretaceous sandstone and shale sequence on the Gilman River. Lithological variation from the same dyke as C-076562. Lake Hazen area.

C-082090: Same dyke as C-082079, 25 m along strike to the west.

C-082750: Basalt flow, Piper Pass locality, Lake Hazen area.

C-076563: Fine grained gabbro sill, south of Wood Glacier, Lake Hazen area.

TABLE 3

Rocks collected from coarse and medium grained sills

Analysis (wt%)	C-082077	C-082078	C-082075	C-082085	C-082076	C-082083	C-082089	C-082084	C-082081
SiO_2	44.00	46.78	48.94	48.98	49.09	45.41	45.56	46.14	48.92
Al_2O_3	13.80	13.48	43.16	11.97	12.73	12.15	13.20	12.61	12.97
Fe_2O_3	4.74	5.48	3.90	5.33	5.80	6.72	6.02	5.49	4.04
FeO	8.60	8.40	10.40	11.50	9.50	8.70	9.70	10.00	9.60
MgO	5.67	5.81	4.57	4.84	3.76	4.98	4.16	4.95	5.31
CaO	7.66	8.16	8.08	9.44	7.65	9.13	8.49	7.70	7.52
Na_2O	3.47	3.80	2.92	2.22	2.72	2.15	3.00	4.55	3.78
K_2O	1.65	.80	1.37	.51	1.43	.73	1.31	.79	.95
TiO_2	3.17	3.04	3.56	3.47	3.93	4.20	4.52	3.58	3.41
P_2O_5	.52	.48	.42	.37	.49	.91	1.00	.35	.34
MnO	.16	.19	.20	.26	.22	.25	.23	.20	.20
CO_2	2.20	0.00	.10	0.00	.10	1.90	.10	.20	.10
H_2O	3.80	3.20	2.10	1.70	2.00	2.40	3.30	3.40	2.80
Total	99.44	99.62	99.72	100.59	99.42	99.63	100.59	99.96	99.94
Ni(ppm)	42.47	52.25	36.36	56.25	29.49	41.91	33.75	69.05	42.59
Cr(ppm)	21.23	32.43	19.83	21.25	10.26	36.03	13.75	15.48	16.67
Zr(ppm)	240	210	280	220	260	260	240	230	180
Norm (cation equivalent)									
Q or (*Ne*)	0.000	0.000	3.502	6.983	7.570	9.311	2.800	(2.217)	.501
Or	10.187	4.994	8.501	3.206	9.002	4.606	8.216	4.912	5.901
Ab	32.561	35.851	27.415	21.038	26.000	20.487	28.643	39.179	35.531
An	17.968	18.212	19.632	22.387	19.495	22.736	19.932	12.196	16.368
Di	2.182	11.776	9.236	11.068	8.550	3.724	9.848	12.589	10.450
He	.732	5.065	5.838	8.585	4.888	1.373	3.963	6.725	5.349
En	9.613	3.848	8.591	8.577	6.789	12.755	7.310	0.000	10.125
Fs	3.186	1.655	5.430	6.653	3.881	4.701	2.942	0.000	5.182
Fo	4.237	5.321	0.000	0.000	0.000	0.000	0.000	6.020	0.000
Fa	1.404	2.289	0.000	0.000	0.000	0.000	0.000	3.216	0.000
Mt	5.100	4.982	4.272	5.486	6.051	6.342	6.699	5.573	4.428
Il	4.613	4.444	5.193	5.103	5.837	6.227	6.705	5.234	4.973
Ap	1.146	1.047	.910	.814	1.099	2.020	2.238	.773	.741
Cc	5.812	0.000	.265	0.000	.269	5.112	.269	.530	.265
Total	98.741	99.484	98.785	99.900	99.431	99.394	99.565	99.164	99.823

C-082077: Sill intruding upper Paleozoic strata in the northwest limb of the Lake Hazen Synclinorium, Lake Hazen area.

C-082078: Sill intruding upper Paleozoic strata in the northwest limb of the Lake Hazen Synclinorium, Lake Hazen area.

C-082075: Sill intruding upper Paleozoic strata in the northwest limb of the Lake Hazen Synclinorium, Lake Hazen area.

C-082085: Sill intruding the Canyon Fiord Formation north of the Air Force Glacier, Ekblaw Lake area.

C-082076: Sill intruding upper Paleozoic strata, Lake Hazen area.

C-082083: Sill intruding the Heiberg Formation, Ekblaw Lake area.

C-082089: Subdiabasic gabbro, layered sill intruding Heiberg Formation on the west side of the Air Force River Valley, Tanquary Fiord area. The same sill as C-082087 (Table 1).

C-082084: Sill intruding Isachsen Formation, Ekblaw Lake area.

C-082081: Sill intruding Isachsen Formation, Ekblaw Lake area.

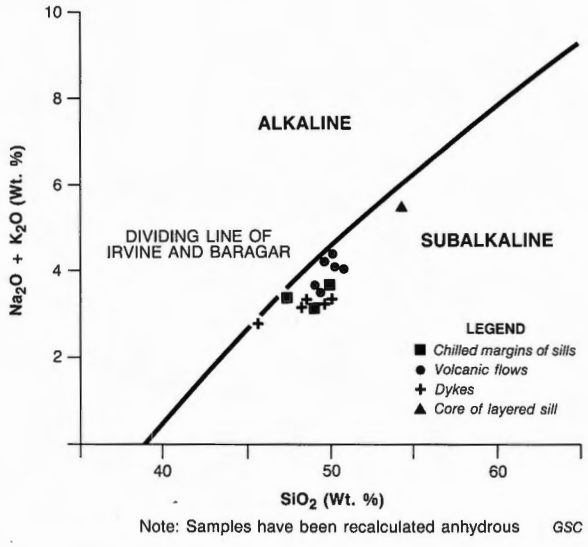

Figure 8. *Total alkali-silica variation diagram indicating the alkaline-subalkaline dividing line of Irvine and Baragar (1971).*

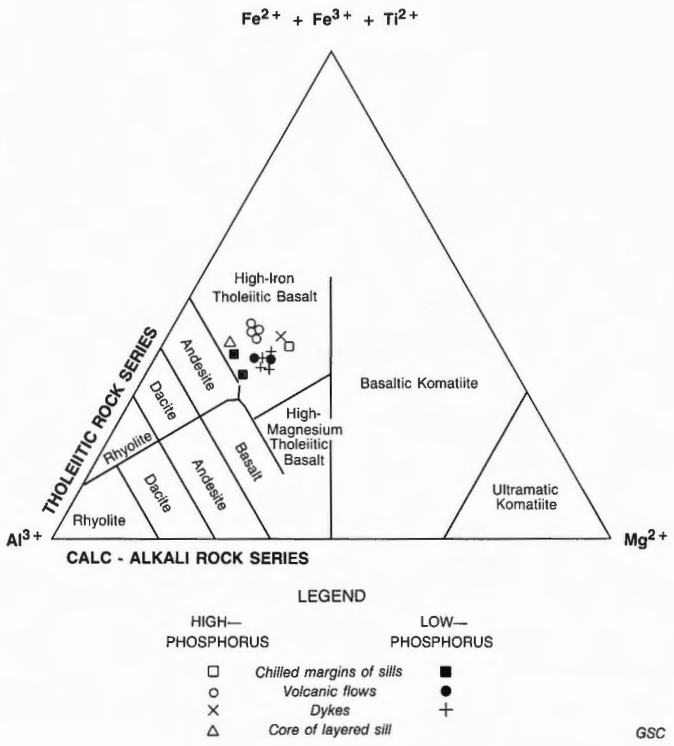

Figure 10. *Cation discrimination diagram of Jensen (1976), distinguishing the samples on the basis of P_2O_5 concentration.*

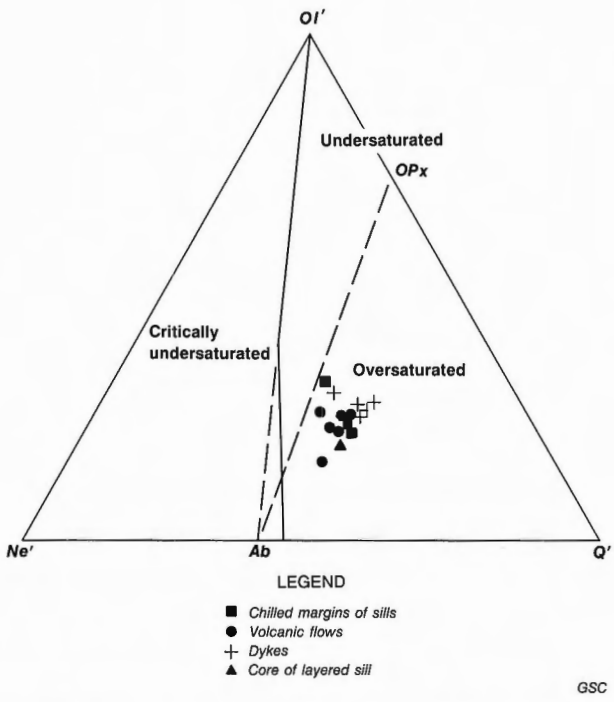

Figure 9. *Basal projection of the* ***Cpx-Ol-Ne-Q*** *tetrahedron showing the alkaline-subalkaline dividing lines of Irvine and Baragar (1971) and the fields of silica saturation.*

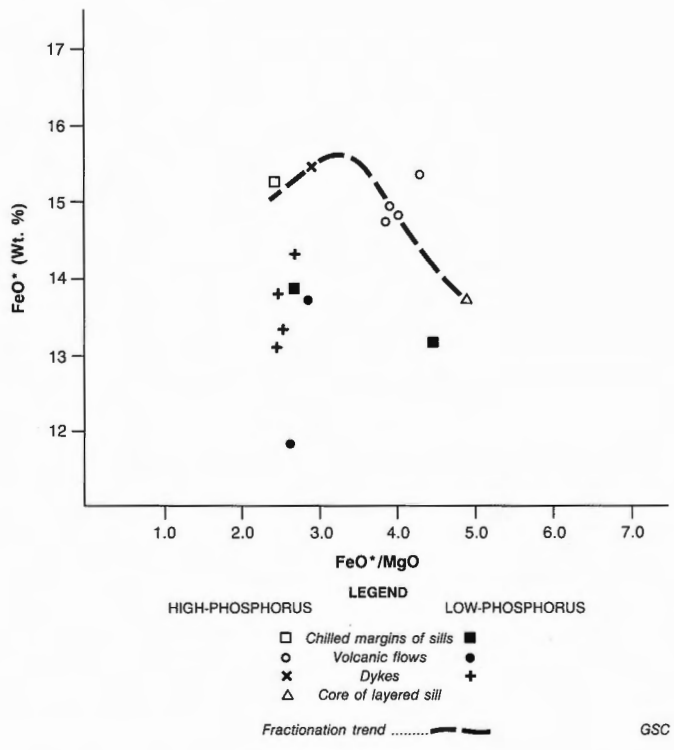

Figure 11. *Total iron-differentiation index (FeO*-FeO*/MgO) diagram of Miyashiro (1974), distinguishing between samples with high and low P_2O_5 concentrations.*

The probable original liquid compositions of these rocks plot in the tholeiitic field of several discriminant diagrams: AFM (Irvine and Baragar, 1971), Jensen cation plot (Jensen, 1976) (Fig. 10), and FeO*/MgO versus FeO* (Fig. 11) and SiO_2 (Fig. 12) diagrams (Miyashiro, 1974). The FeO*/MgO versus FeO* diagram illustrates that the distinction between the high- and low-phosphorus groups is a fundamental character of the suite. The samples representative of the high-phosphorus group show considerable variation in FeO*/MgO ratio and, within the limits of available samples, a relatively well defined trend of iron enrichment. It is concluded that iron enrichment continued until the FeO*/MgO ratio was approximately 3.5. This was followed by a general trend of iron depletion to the composition of the pegmatoid core of the layered sill in the Heiberg Formation, presumably a residual composition. Note that flows were derived from the high-phosphorus magma, past the inferred peak of iron enrichment after considerable fractionation. This is in contrast with the low-phosphorus magma group, most of whose rocks exhibit a restricted range of FeO*/MgO ratios, between 2.5 and 3.0, and proportionally lower FeO* (<14.5) for a given FeO*/MgO ratio than the high-phosphorus compositions. Apparently flows were derived from the low-phosphorus magma without an observable crustal fractionation/iron enrichment trend analogous to that exhibited by the flows originating from high-phosphorus sources. Because of the generally narrower range of FeO*/MgO composition of the low-phosphorus magma, a trend of iron enrichment was not developed. However, one low-phosphorus sample – from a thin hypabyssal sill intruding the Christopher Formation (C-082080), and with an FeO*/MgO ratio of 4.5 – suggests that some fractionation of the low-phosphorus magma did take place. Silica (Fig. 12) does not exhibit a clearly discernible relationship with variations in the FeO*/MgO ratio for low-phosphorus compositions, although a progressive increase in SiO_2 is developed in high-phosphorus compositions past the inferred peak of iron enrichment. Based on these criteria, it is concluded that the suite represents subalkaline basic volcanic rocks with tholeiitic rock series affinities.

The low concentration of MgO and the generally high total iron of all samples is notable. Mg values for the most primitive observable low-phosphorus and high-phosphorus magmas are 57.5 and 47.4 respectively. This in itself suggests that the most primitive, observable compositions do not represent primary magmas, and that all magmas penetrating exposed crustal levels were derived by fractionation of parental magmas at depths greater than five kilometres (1.5 kb). This inference is supported by available trace element data. These two constraints are employed below to produce simple models of approximate parental compositions for the low- and high-phosphorus magmas.

Minor elements

Two minor elements, phosphorus and titanium are of particular interest. As discussed above, in the section on major elements, the variation of phosphorus with silica indicates a partition of the suite into two groups, those rocks having in excess of 0.9 wt % P_2O_5 (~4000 ppm phosphorus) and those having less (Fig. 13). There is no indication of any transition between the two groups. High-phosphorus compositions were revealed through the analysis of samples collected from a restricted number of igneous bodies. The basalt flows are well represented by four samples, derived from all the flows, except the lowermost one, at Piper Pass. The layered sill in the Heiberg Formation also belongs to the high-phosphorus group, as does one dyke cutting the Jurassic-Cretaceous sedimentary sequence, in shales just above the

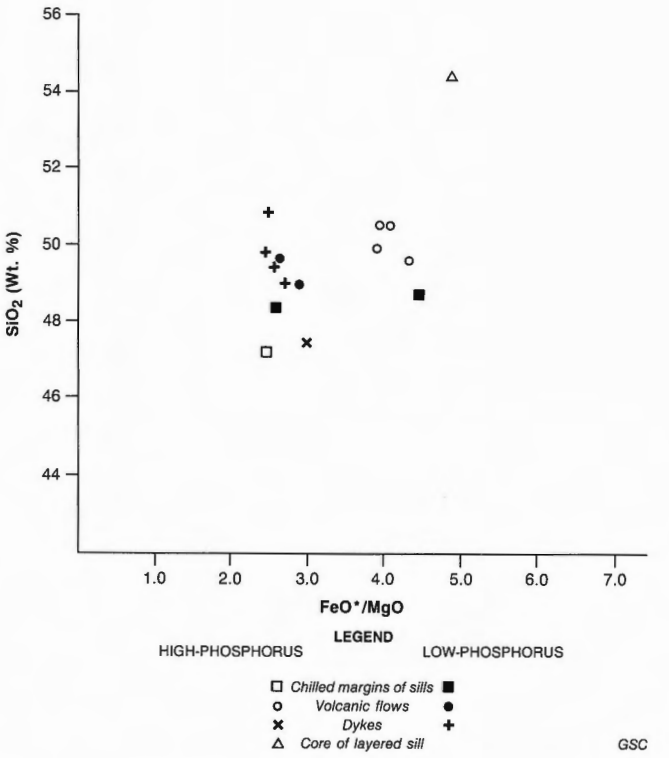

Figure 12. *Silica-differentiation index (SiO_2-FeO*/MgO) diagram of Miyashiro (1974).*

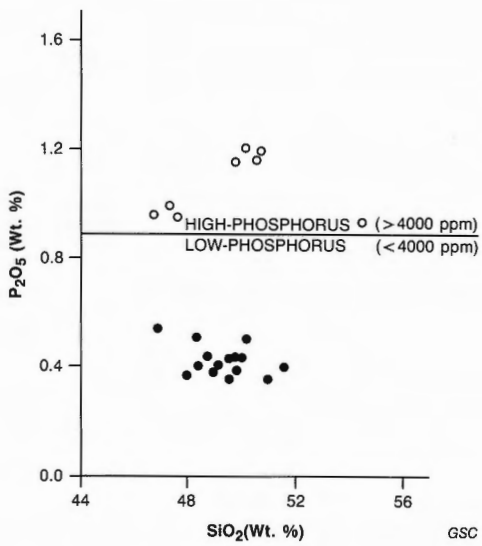

Figure 13. *Phosphorus-silica variation diagram, indicating the separation of the suite into two distinct magmas about a dividing line chosen at 4000 ppm phosphorus.*

Heiberg Formation. Excluding certain of the sills sampled, these rocks represent evolved liquid compositions of the high-phosphorus group. Other samples have the composition of the low-phosphorus magma. Distinctions between the two groups are also shown by the TiO_2 vs. FeO*/MgO variation diagram (Fig. 14). All compositions are highly evolved (FeO*/MgO>2.0) and enriched in titanium (TiO_2>3.0).

Comparison of flows representing the two groups indicates that although they have similar abundances of TiO_2, between 3 and 4 weight per cent, they had very different crystallization histories. As suggested above, low-phosphorus flows were derived earlier in the fractionation history of the magma and have compositions similar to several dykes and the chilled margins of some sills. High-phosphorus flows, on the other hand, were derived late in the fractionation history of the high-phosphorus magma. The high-phosphorus magma which initially entered the upper crust (Sverdrup Basin), is probably represented by the chilled margin of the layered Heiberg sill. The high phosphorus composition continued to enrich TiO_2 in the melt until FeO*/MgO reached about 3.5. Following this, TiO_2 in the melt was substantially depleted, probably by the crystallization of oxide phases resulting in residual liquids with low concentrations of TiO_2, as represented by both the flows and the leucogabbro of the layered sill. The later derivation of flows from sills fractionating high in the crust is consistent with the stratigraphic observation that high-phosphorus flows are stratigraphically younger than the low-phosphorus flow unit, and with the observed variation of FeO* relative to the FeO*/MgO ratio. All the above trends are consistent with, and fall exclusively in, the fields characteristic of the crustal fractionation of tholeiitic magmas.

Trace elements

The trace element data for this study were determined by optical spectrometry and the analyses have large associated uncertainties (R.M. Meeds, pers. comm., 1980). Nevertheless, certain elements exhibit consistent abundance and qualitatively correct variation trends and may be used to corroborate a petrogenetic scheme deduced from the major elements and stratigraphic relationships. Four trace elements are considered: Ni, Cr, Sr and Zr. Two trace element determinations considered very reliable are for Ni and Cr. Both exhibit a strong positive correlation with MgO (Fig. 15). Sample analysis indicates that the Ni/Cr ratios of the liquid compositions hover around 2:1, although some samples have values as low as 1:1.3. Consideration of the large analytic uncertainty, ±20 per cent of the observed abundances, could easily accommodate this variation. Tables 1 and 2 indicate that the least fractionated liquid compositions (i.e. the samples having the lowest FeO*/MgO ratios) have abundances of Ni between 40 and 50 ppm with Cr generally between 23 and 36 ppm. For Ni, this is ten times lower than the concentrations commonly observed in unfractionated basaltic magmas (Prinz, 1967; p. 302).

Although Sr values were obtained by optical spectrometry, they are not considered sufficiently reliable to be reported.

Zirconium exhibits no discernible variation trends with other elements. Zirconium is used only to ascertain the ratio of Zr/P_2O_5, and differences in P_2O_5 abundance within the suite outweigh the effects of any uncertainty in the Zr abundances for determining this ratio.

Discussion

The basic igneous rocks of the study area comprise a suite of dykes, sills and flows that were intruded and extruded in the Sverdrup Basin during mid-Cretaceous time. Tertiary deformation has exposed a crustal thickness of five

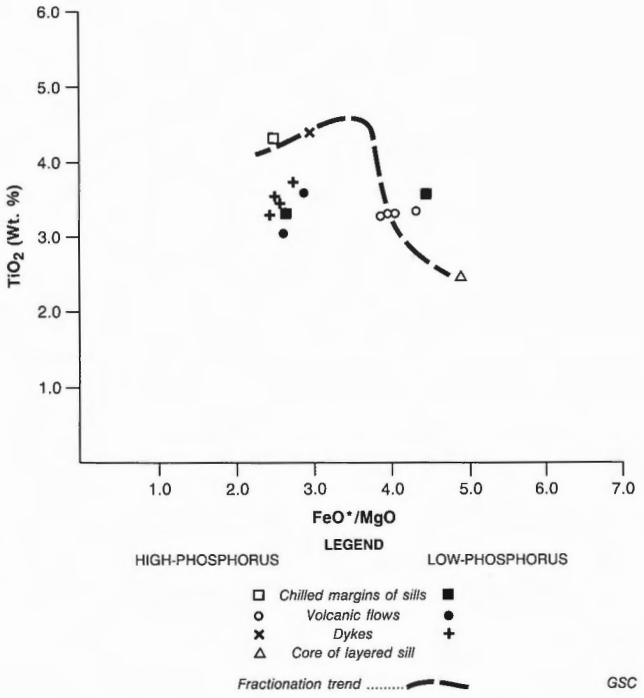

Figure 14. *Titania-differentiation index (TiO_2-FeO*/MgO) diagram of Miyashiro (1974) distinguishing between the high- and low-phosphorus compositions.*

kilometres (1.5 kb) (Osadetz, 1982) below the late Albian-Cenomanian accretion surface of the Hassel Formation. A few feeder dykes pass through the penetratively deformed lower Paleozoic strata, giving rise to a complex of sills which in turn source a swarm of dykes in the Sverdrup Basin (<2.5 km). The emplacement of these intrusions is inferred to be coeval with the extrusion of volcanic flows in the Hassel Formation at Lake Hazen.

All samples fall within the subalkaline field of the alkali-silica variation diagram (Fig. 8) and all plot within the *Q'-Opx-Ab* subzone of the *Ol'-Ne'-Q'* basal projection of the *Cpx-Ol-Ne-Q* tetrahedron (Fig. 9). The entire suite plots within the tholeiitic field of several discriminant diagrams for subalkaline rocks (Figs. 10, 11, 12, 14). The inferred tholeiitic rock series affinities are consistent with the petrography of the suite.

Minor element data indicate that two distinct magmas are represented in the suite. The two compositions are distinguished by their P_2O_5 content. Samples having $P_2O_5 \geq .90$ weight per cent (~4000 ppm P) form a separate group distinct from samples having lesser P_2O_5 (Fig. 13). Using this distinction it is possible to discern a trend of iron enrichment (Fig. 11) which accompanied fractionation of the P_2O_5-rich magma, starting from a composition similar to that of the chilled margin samples from the layered sill in the Heiberg Formation (C-082087, see Table 1). The variation of TiO_2 with FeO*/MgO is observed to mimic that of FeO* for the high-phosphorus magma (Fig. 14). These diagrams indicate that the high-phosphorus magma reached a peak of iron enrichment at FeO*≈15.5 weight per cent and FeO*/MgO≈3.5, and that a similar peak of enrichment in titania was encountered. It is noteworthy that the flows derived from the high-phosphorus magma represent liquids fractionated past the peak of iron and titanium enrichment.

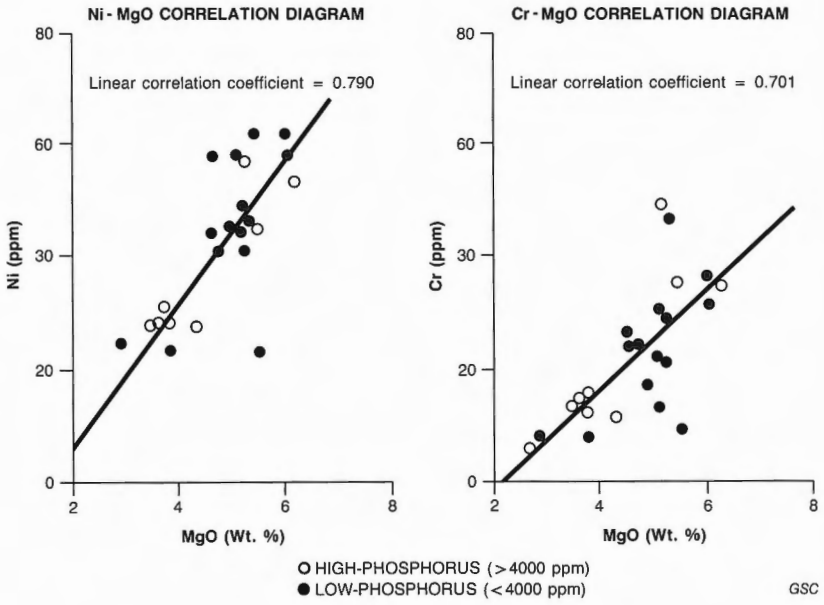

Figure 15. *Trace element variations with MgO. 15a: Ni-MgO. 15b: Cr-MgO.*

This is in contrast with the other, low-phosphorus, magma; the flows derived from which represent the least fractionated compositions (Table 2; Figs. 11, 14). In this case, data do not support a shallow crustal iron enrichment trend because the low-phosphorus magma was extruded shortly after or immediately upon reaching shallow crustal levels (<5 km; 1.5 kb). This is consistent with observed stratigraphic relationships amongst flow units.

Major element data suggest that these rocks were extensively fractionated when they intruded exposed crustal levels. Fe^{2+}/Mg ratios indicate that the most primitive compositions represent magmas not in equilibrium with mantle olivine ($Fo_{90}Fa_{10}$). The least fractionated compositions are best represented by the chilled margin of the high-phosphorus sill (C-082087, Table 1) and a low-phosphorus flow south of the Piper Pass (C-082750, Table 2). In both cases the original liquids were depleted in MgO, Ni and Cr, and enriched in FeO* and TiO_2 in comparison to several common unfractionated basalt compositions (Irvine and Baragar, 1971). Two factors suggest that the original liquids achieved their observed compositions by fractional crystallization at relatively low pressures in the crust. The first factor involves the observation that olivine was a liquidus phase in the low-phosphorus magma when the first flow was extruded. The second factor is the relative depletion of MgO, Ni and Cr and the enrichment of FeO* and Fe^{2+} in the least fractionated compositions.

Presumably these liquids were derived by the primary fractionation of olivine and other phases. The removal of plagioclase is inferred because it too is a phenocryst phase. The depletion of Cr may have resulted from the crystallization of either clinopyroxene or Cr-spinel.

If the initial concentration of Ni in the parental magma was in the order of 400-500 ppm, then simple Rayleigh fractionation would suggest that the low-phosphorus volcanic flow (C-082750, Table 2) could be derived by the fractionation of approximately 20 per cent olivine, if olivine was the only phase fractionating Ni. This produces a model of a parental magma composition with Fe^{2+} and Mg contents that are in rough equilibrium with a mantle olivine ($Fo_{90}Fa_{10}$). This must be considered an upper limit for olivine fractionation from the parental low-phosphorus magma. Addition of other femic phases, most likely clinopyroxene (of suitable composition), could also move the observed low-phosphorus magma toward equilibrium with a mantle source. As the contribution of clinopyroxene fractionation is increased the amount of olivine fractionation can be decreased and the weight fraction of the residual liquid (the observed composition) decreases. Lack of knowledge of the composition of crystallizing phases prevents a quantitative modelling of this process. Fractionation of plagioclase does not alter the Fe^{2+}/Mg ratio yet it does serve to decrease its weight fraction in the residual liquid (the observed composition).

The addition of approximately 20 per cent of a similar olivine ($Fo_{80}Fa_{20}$) to the high-phosphorus magma does not give a parental magma in equilibrium with $Fo_{90}Fa_{10}$, nor a suitable Mg-value, because of its higher Fe^{2+} content. Only larger amounts of olivine fractionation could bring the high-phosphorus composition (C-082087) into equilibrium with $Fo_{90}Fa_{10}$; however, this is not supported by the Ni concentrations in the derivative liquid (Ni = 50 ppm). Another femic mineral, probably clinopyroxene, needs to be added to bring the composition of the high-phosphorus magma into equilibrium with a mantle source. Again, lack of knowledge of the composition of fractionating phases prevents calculation of the degree of fractionation required to produce an appropriate parental magma composition.

Tertiary structure indicates that the fractionation chambers must have been at depths greater than five kilometres (1.5 kb) at the time of intrusion (Osadetz, 1982). With qualifications, some experimental work suggests that the crystallization of olivine, under anhydrous conditions, is suppressed at pressures greater than 13.5 kilobars (~46 km) (Ringwood, 1975). This is within the range of crustal thicknesses documented for the Sverdrup Basin in seismic refraction studies. Sobczak (1963) suggested that a large basic pluton, approximately 2400 m thick and 13 km wide, is present under Amund Ringnes Island at a depth of 15 km. This is another location where volcanic rocks occur in the Hassel Formation (Balkwill, 1983). Although the correlation is tenuous the data suggest that mid-Cretaceous basic magmatism was characterized by original intrusion into lower crustal levels (5 km < depth of primary fractionation < 46 km), where fractionation of the parental tholeiitic basalts occurred prior to the final intrusion of the magmas into the sediments of Sverdrup Basin.

The petrological significance of the distinction between the low-phosphorus/high-phosphorus magmas remains to be discussed. Watson (1980) argued that mantle source regions probably contained 200 ppm ± 100 ppm phosphorus, if the bulk solid/liquid partition coefficient, D (controlling the distribution of P_2O_5 in melts produced by equilibrium melting of the mantle), lies between D=0.03 and D=0.01. He also suggested that small degrees of partial melting (>3.5%) would completely remove phosphorus from the source. When applied to this suite, the latter conclusion indicates that the mantle source regions for these magmas were not previously depleted, and that the arguments for supporting the fractionation models based on trace elements, as discussed above, are reasonable.

If a model bulk composition of the parental low-phosphorus magma is calculated (assuming 20% $Fo_{80}Fa_{20}$ fractionation), the parental model would contain P_2O_5=0.2 weight per cent. On a diagram similar to Watson's, the P_2O_5

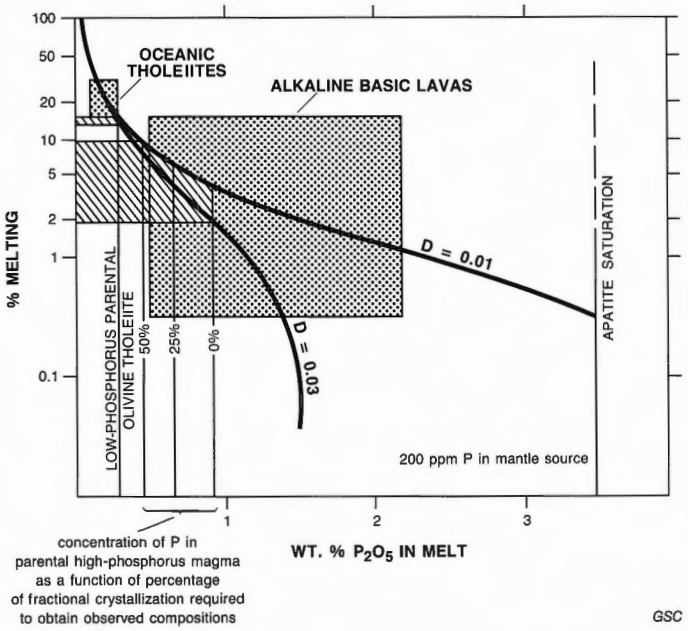

Figure 16. *Concentration of P_2O_5 in the melt as a function of both degree of partial melting of a mantle source (200 ppm P) and bulk solid/liquid distribution coefficients for equilibrium partial melting (after Watson, 1980).*

abundance in this parental liquid has been plotted to exhibit the percentage of batch melting of a 200 ppm P mantle source region for a reasonable range of bulk solid/liquid partition coefficients (Fig. 16). Notice that the low-phosphorus magma plots very near the field for oceanic tholeiites. It is suggested that the degree of partial equilibrium melting needed to form this magma is about 12 per cent. At this level of partial melting, phosphorus in the source region would be entirely consumed.

Because the primary fractionation history of the high-phosphorus magma (C-082087) is uncertain, the bulk composition of the parental magma is also uncertain. Yet, the distinctive P_2O_5 abundance in the high-phosphorus rocks is so great as to remain distinguishable over a wide range of fractionation histories. If the observed composition (C-082087) represents a residual liquid ranging from 100-50 per cent by weight of the original magma, the degree of partial equilibrium melting required to form this magma would range between nine and two per cent (Fig. 16). Note also that this magma plots in the field commonly occupied by alkaline basic rocks. Within a restricted range of these various degrees of partial equilibrium melting, residual apatite may remain in the residual mantle to affect the partition of trace and minor elements into the melt (Watson, 1980).

Recognizing that the calculations discussed here are only approximate, and that only semi-quantitative inferences may be made, it is proposed that these two parental magmas were derived from an undepleted mantle source region, with average phosphorus concentrations, by different degrees of partial melting of separate portions of the source.

It is not possible to determine which parental magma was generated first, only that flows derived from the low-phosphorus magma by at least one stage of crustal fractionation were extruded first. The high-phosphorus magma was derived by substantially less melting of a similar source, and this magma underwent at least two stages of crustal fractionation before flows were extruded from it. It is of note that the low-phosphorus magma, which is the result of a greater degree of partial melting, forms substantially more sills and dykes, and is presumably volumetrically more abundant than the high-phosphorus magma, which is known to form only one sill; volumetrically, the sills represent the bulk of the rock formed by the entire suite.

Tectonic setting

Flows in the late Albian-early Cenomanian Hassel Formation are thin and widely distributed. As discussed above, they are aligned parallel to the present continental margin. Just as the suite of intrusive rocks at Tanquary Fiord is considered to have been contemporaneous with volcanic flows at Lake Hazen, most basic plutonism in Sverdrup Basin is probably coeval with known flows and occurred over a much narrower time interval than previously suggested by Balkwill (1978). Jackson (in Jackson and Halls, 1983) reported that all sills sampled from a 10 km thick stratigraphic section (Early Triassic to early Late Jurassic) at Buchanan Lake, Axel Heiberg Island, yield Early Cretaceous paleopoles. Both stratigraphic and paleomagnetic evidence point toward a limited period of basic igneous activity, suggesting that K/Ar ages older than Early Cretaceous should be re-evaluated.

Reconstruction of the pre-Tertiary cratonic configuration indicates that northern Ellesmere Island, Northern Greenland and Svalbard formed conterminous tectonic blocks. In Svalbard, erosion has exposed extensive sills and dykes of Late Jurassic to late Early Cretaceous age (Burov and others, 1977). In Franz Josef Land, basalt flows, roughly correlative with the Mesozoic Sverdrup Basin volcanics, were extruded in a similar stratigraphic setting to the flows in the Isachsen Formation at Bunde Fiord (Nalivkin, 1973, p. 393). Analyses of these rocks (Tyrrell and Sandford, 1933) indicated that they are also iron-enriched tholeiitic basalts, quite similar to the Lake Hazen flows. The TiO_2 content of the Franz Josef rocks may have been underestimated by the older methods of analysis (cf. Weigand and Testa, 1982).

In Northern Greenland, a Late Cretaceous (66 Ma) basic dyke swarm intrudes strata as young as Early Cretaceous (Soper and others, 1982). The younger rocks of northern Greenland are distinctly different from those of the Barents Shelf – Ellesmere Island area. Volcanic rocks of the Barents Shelf and Sverdrup Basin are distinguished as subalkaline on both the total alkali-silica variation diagram and the basal projection of the *Cpx-Ol-Ne-Q* tetrahedron. The dyke swarm of Northern Greenland clearly plots in the alkaline field of the total alkali-silica diagram (Soper and others, 1982). The compositions of most volcanic rocks from Northern Greenland plot in the *Ol'-Opx-Ab* zone of the basalt tetrahedron, although some samples are marginally critically undersaturated or oversaturated. A genetic relationship between the medial Cretaceous rocks of the Ellesmere Island – Barents Shelf tholeiitic suite and the latest Cretaceous alkaline suite of Northern Greenland is precluded by age alone. Similarly, both the high content of alkalies (>3.0 wt %) and low Ni (<56 ppm) reported for the Greenland rocks (Soper and others, 1982) preclude the derivation of the

Ellesmere-Barents tholeiitic rocks from an older magma similar in composition to the magmas of the Northern Greenland event. Considering the somewhat alkaline minor and trace element characteristics of the parental high-phosphorus model magma, it may be worth investigating to see if the alkaline suite could have been derived by a moderate pressure (13-18 kb) fractionation of a tholeiitic parental magma, as described by Ringwood (1975, p. 137). It is appropriate to note here that the high concentrations of TiO_2 and P_2O_5 utilized by Soper and others (1982) to indicate alkali affinities in the Greenland suite (cf. Floyd and Winchester, 1975), do not serve to distinguish the alkaline rocks from the high-iron tholeiites of the Sverdrup Basin suite (Fig. 17). This observation may be valuable to those attempting to determine rock series affinities in altered suites containing high TiO_2.

Like the Sverdrup Basin tholeiites, the Barents Shelf tholeiites are enriched in iron and titanium (Weigand and Testa, 1982). Phosphorus abundances in the Barents Shelf suite resemble the low-phosphorus compositions of the Lake Hazen rocks. As in the case of the Barents Shelf suite, all of the low-phosphorus compositions of the Lake Hazen volcanics plot within the oceanic field of the K_2O-TiO_2-P_2O_5 discriminant diagram of Pearce and others (1975) (Fig. 18). In contrast, the high-phosphorus compositions from Ellesmere Island plot in the continental field of the same diagram. With increasing fractionation, the high-phosphorus compositions outline a trend that is parallel to that described for dolerites that occur on the margins of North America (Weigand and

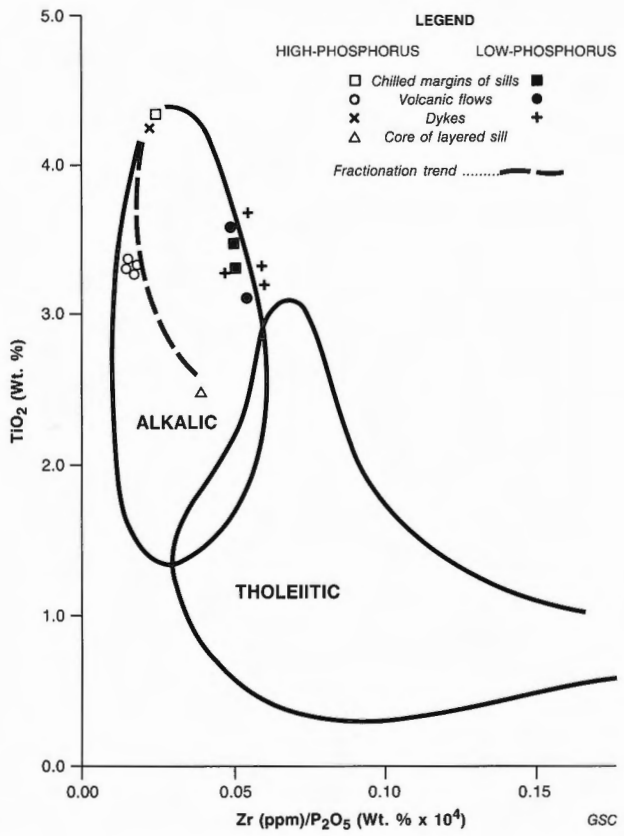

Figure 17. *Alkalic-tholeiitic discriminant diagram of Floyd and Winchester (1975).*

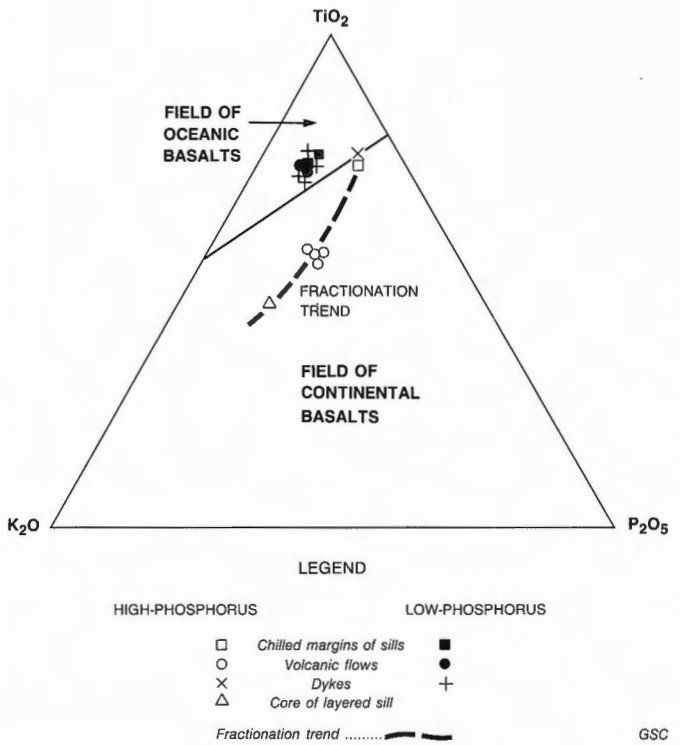

Figure 18. *Tectonic setting diagram of Pearce and others (1975).*

Ragland, 1970). Pearce and others (1975) observed that other doleritic suites distributed across the two fields were intruded in continental crustal settings that could be spatially and temporally associated with the formation of divergent plate boundaries.

Intrusion of the Barents Shelf – Sverdrup tholeiites precedes any spreading on the Nansen – Gakkel Ridge that is no older than anomaly 27 time (61 Ma) (Feden and others, 1979; Soper and others, 1982). Sverdrup tholeiites cannot be accommodated within the concentric subsidence model of Balkwill (1978). Instead, stratigraphic and paleogeographic considerations suggest that basic magmatism of Late Jurassic to early Late Cretaceous age must have paralleled the future edge of the Amerasian Basin. This is generally consistent with several models for the formation of the Amerasian Basin (Newman and others, 1977; Sweeney and others, 1978) although at considerable odds with other interpretations (Herron and others, 1974).

The timing of events during the opening of the Amerasian Basin cannot be accurately determined using data from the ocean basin. Embry (1985) proposes using unconformity bounded, cratonic, stratigraphic sequences to date events in the adjacent ocean basin. Using these sequences in this way, basic volcanism in late Albian-Cenomanian time would have occurred during a period of cratonic uplift, accompanying the later stages of seafloor spreading prior to the thermal subsidence of the craton margin.

Conclusions

1. Volcanic rocks in the Hassel Formation on northern Ellesmere Island, and their associated intrusives, were derived by partial melting of similar mantle source regions. The original mantle source regions probably did not contain anomalous amounts of phosphorus or nickel. Nevertheless, two distinct parental olivine tholeiite magmas appear to have been involved. One parental olivine tholeiite magma is characterized by a lower content of phosphorus and titanium. To some extent it resembles an oceanic tholeiite (Figs. 16, 18) and was derived by ~12 per cent partial melting of a mantle source region. The other parental magma, also an olivine tholeiite, is very similar to the first, except for its higher phosphorus and titanium concentrations, and was probably derived by two to nine per cent batch melting of the mantle. It exhibits characteristics of those continental tholeiitic basalts that have slight alkaline tendencies.

2. Both parental magmas were intruded into a thick, continental crust where they underwent low pressure (1.5-13.5 kb; 5-46 km) fractionation of olivine ± clinopyroxene and plagioclase. These fractionated liquids are the most primitive compositions now represented by exposed rocks.

3. Fractionated parental liquids were intruded into the shallow crust at a depth of 2.5 to 1.0 km below the surface, where they formed a suite of sills and flows in sedimentary strata of the Sverdrup Basin.

4. The low-phosphorus magma was extruded as flows without further fractionation. The high-phosphorus magma continued to fractionate in the shallow crust, possibly at depths of less than 2.5 km, along a pronounced trend of iron and titanium enrichment. Flows were derived from this magma only after it passed the peak of iron and titanium enrichment. These flows occur stratigraphically above the low-phosphorus flows.

5. This volcanic suite is similar to the Cretaceous dolerites of Svalbard. There are temporal and spatial reasons to believe that both suites represent a major intrusive event that was associated with continental rifting and the formation of the Amerasian Basin. Specifically, these magmas were extruded prior to thermal subsidence of the craton during the later stages of seafloor spreading.

Acknowledgments

Fieldwork for this project was supported by the Institute of Sedimentary and Petroleum Geology and the Polar Continental Shelf Project of the Geological Survey of Canada, Department of Energy, Mines and Resources. Dr. A.F. Embry directed the party in the field and Dr. T. Frisch expedited the analysis of the samples in Ottawa. This manuscript benefitted from the process of internal scientific review. In particular, the authors wish to thank Dr. W.R.A. Baragar for his helpful suggestions.

REFERENCES

Abbey, S.
1979: Rock analysis: methods at the Geological Survey of Canada; Geostandards Newsletter, v. 3, no. 1, p. 97-101.

Balkwill, H.R.
1983: Geology of Amund Ringnes, Cornwall and Haig-Thomas islands, District of Franklin; Geological Survey of Canada, Memoir 390, 76 p.

1978: Evolution of Sverdrup Basin, Arctic Canada; American Association of Petroleum Geologists Bulletin, v. 62, no. 6, p. 1004-1028.

Balkwill, H.R. and Fox, F.G.
1982: Incipient rift zone, western Sverdrup Basin, Arctic Canada; in Arctic Geology and Geophysics, A.F. Embry and H.R. Balkwill (eds.); Canadian Society of Petroleum Geologists, Memoir 8, p. 171-188.

Blackadar, R.G.
1964: Basic intrusions of the Queen Elizabeth Islands, District of Franklin; Geological Survey of Canada, Bulletin, v. 97, 37 p.

Burov, Yu.P., Krasil'scikov, A.A., Firsov, L.V., and Klubov, B.A.
1977: The age of the Spitsbergen dolerites; Norsk Polarinstitutt Årbok 1975, p. 101-108.

Christie, R.L.
1964: Geological reconnaissance of northeastern Ellesmere Island, District of Franklin; Geological Survey of Canada, Memoir 331, 79 p.

Embry, A.F.
1985: Mesozoic stratigraphy of Canadian Arctic Archipelago and implications for opening of Amerasian Basin (abstract); American Association of Petroleum Geologists Bulletin, v. 69 no. 2, p. 253.

Feden, R.H., Vogt, P.R., and Fleming, H.S.
1979: Magnetic and bathymetric evidence for the "Yermak hot spot" northwest of Svalbard in the Arctic Basin; Earth and Planetary Science Letters, v. 44, p. 18-38.

Floyd, P.A. and Winchester, J.A.
1975: Magma type and tectonic setting discrimination using immobile elements; Earth and Planetary Science Letters, v. 27, p. 211-218.

Fricker, P.E.
1963: Geology of the expedition area, western central Axel Heiberg Island, Canadian Arctic Archipelago; in Jacobs-McGill Arctic Research Expedition 1959-1962, Geology No. 1, Axel Heiberg Island Research Reports, 156 p.

Herron, E.M., Dewey, J.F., and Pitman, W.C.
1974: Plate tectonics model for the evolution of the Arctic; Geology, v. 2, p. 377-380.

Irvine, T.N. and Baragar, W.R.A.
1971: Guide to the chemical classification of the common volcanic rocks; Canadian Journal of Earth Science, v. 8, p. 523-548.

Jackson, K.C. and Halls, H.C.
1983: A paleomagnetic study of igneous rocks of the Sverdrup Basin; Canadian Arctic Archipelago (abstract), GAC-MAC-CGU 1983 Joint Meeting Victoria, Program with Abstracts, v. 8, 84 p.

Jensen, L.S.
1976: A new cation plot for classifying subalkalic volcanic rocks; Ontario Division of Mines, Miscellaneous Paper 66, 22 p.

Lorenz, V., McBirney, A.R., and Williams, H.
1970: An investigation of volcanic depressions: Part III, Maars, tuff rings, tuff cones and diatremes; University of Oregon, Centre for Volcanology, Eugene, Oregon.

Miall, A.D.
1979: Tertiary fluvial sediments in the Lake Hazen intermontane basin, Ellesmere Island, Arctic Canada; Geological Survey of Canada, Paper 79-9, 25 p.

Miyashiro, A.
1974: Volcanic rock series in island arcs and active continental margins; American Journal of Science, v. 274, p. 321-355.

Nalivkin, D.V.
1973: Geology of the U.S.S.R., translated by N. Rast; Oliver and Boyd, Edinburgh, 855 p.

Newman, G.W., Mull, C.G., and Watkins, N.D.
1977: Northern Alaskan paleomagnetism, plate rotation, and tectonics (abstract); Alaska Geologic Society, Symposium, Anchorage, Alaska, p. 16-19.

Osadetz, K.G.
1982: Eurekan structures of the Ekblaw Lake area, Ellesmere Island, Canada; in Arctic Geology and Geophysics, A.F. Embry and H.R. Balkwill (eds.); Canadian Society of Petroleum Geologists, Memoir 8, p. 219-232.

Pearce, T.H., Gorman, B.E., and Birhett, T.C.
1975: The TiO_2-K_2O-P_2O_5 diagram: a method of discriminating between oceanic and non-oceanic basalts; Earth and Planetary Science Letters, v. 24, p. 419-426.

Plauchut, B.P.
1971: Geology of the Sverdrup Basin; Bulletin of Canadian Petroleum Geology, v. 19, p. 659-679.

Prinz, M.
1967: Geochemistry of basaltic rocks: trace elements; in Basalts, Volume 1, H.H. Hess and A. Poldervaart (eds.); Interscience, New York, p. 271-324.

Ricketts, B., Osadetz, K.G., and Embry, A.F.
1985: Volcanic style in the Strand Fiord Formation (Upper Cretaceous), Axel Heiberg Island, Canadian Arctic Archipelago; Polar Research; v. 3 n.s., no. 1, p. 107-122.

Ringwood, A.E.
1975: Composition and petrology of the Earth's mantle; McGraw Hill, 618 p.

Sobczak, L.W.
1963: Regional gravity survey of the Sverdrup Islands and vicinity with map: no. 11 - Sverdrup Islands; Earth Physics Branch, Ottawa, 19 p.

Soper, N.J., Dawes, P.R., and Higgins, A.K.
1982: Cretaceous-Tertiary magmatic and tectonic events in north Greenland and the history of adjacent ocean basins; in Nares Strait and the drift of Greenland: a conflict in plate tectonics, P.R. Dawes and J.W. Kerr (eds.); Meddelelser om Grønland, Geoscience, v. 8, p. 205-220.

Stott, D.F.
1969: Ellef Ringnes Island, Canadian Arctic Archipelago; Geological Survey of Canada, Paper 68-16, p.

Sweeney, J.F., Irving, E., and Geuer, J.W.
1978: Evolution of the Arctic Basin; in Arctic Geophysical Review, J.F. Sweeney (ed.); Earth Physics Branch, Canada, v. 45, no. 4, p. 91-100.

Thorsteinsson, R.
1974: Carboniferous and Permian stratigraphy of Axel Heiberg and western Ellesmere Island, Canadian Arctic Archipelago; Geological Survey of Canada, Bulletin 224, 115 p.

1971: Strand Fiord, District of Franklin; Geological Survey of Canada, Map 1301A.

Thorsteinsson, R. and Trettin, H.P.
1969: Bukken Fiord, District of Franklin; Geological Survey of Canada, Map 1310A.

Tozer, E.T.
1963: Mesozoic and Tertiary stratigraphy, western Ellesmere Island and Axel Heiberg Island, District of Franklin (Preliminary Account); Geological Survey of Canada, Paper 63-30, 38 p.

Trettin, H.P., Mayr, U., Embry, A.F., and Christie, R.L.
1982: Preliminary geological map and notes. Part of Lady Franklin Bay map area, District of Franklin (NTS 120C); Geological Survey of Canada, Open File Report 834.

Tyrrell, G.W. and Sandford, K.S.
1933: Geology and petrology of the dolerites of Spitsbergen; Transactions of the Royal Society of Edinburgh, v. 43, p. 254-321.

Watson, E.B.
1980: Apatite and phosphorus in mantle source regions: an experimental study of apatite/melt equilibria at pressures to 25 kbar; Earth and Planetary Science Letters, v. 51, p. 322-335.

Weigand, P.W. and Ragland, P.C.
1970: Geochemistry of Mesozoic dolerite dykes from eastern North America; Contributions to Mineralogy and Petrology, v. 29, p. 195-214.

Weigand, P.W. and Testa, S.M.
1982: Petrology and geochemistry of Mesozoic dolerites from the Hinlopenstretet area, Svalbard; Polar Research, v. 1, p. 35-51.